J. Phys. A: Math. Gen. 28 (1995) 6567–6584. Printed in the UK

Generalized viscoelastic models: their fractional equations with solutions

H Schiessel†, R Metzler‡, A Blumen† and T F Nonnenmacher‡

† Theoretical Polymer Physics, University of Freiburg, Rheinstrasse 12, D-79104 Freiburg, Germany

‡ Department of Mathematical Physics, University of Ulm, Albert-Einstein-Allee 11, D-89069 Ulm/Donau, Germany

Received 24 July 1995

Abstract. Recently fractional calculus (FC) has encountered much success in the description of complex dynamics. In particular FC has proved to be a valuable tool to handle viscoelastic aspects. In this paper we construct fractional rheological constitutive equations on the basis of well known mechanical models, especially the Maxwell, the Kelvin–Voigt, the Zener and the Poynting–Thomson model. To this end we introduce a fractional element, in addition to the standard purely elastic and purely viscous elements. As we proceed to show, many of the fractional differential equations which we obtain by this construction method admit closed form, analytical solutions in terms of Fox H-functions of the Mittag–Leffler type.

1. Introduction

Relaxation processes deviating from the classical exponential (Debye) behaviour are often encountered in the dynamics of complex materials. In many cases experimentally observed relaxation functions exhibit a stretched exponential (Kohlrausch–Williams–Watts) decay [1, 2]

$$\Phi(t) \propto \exp(-(t/\tau)^{\alpha}) \tag{1}$$

with $0 < \alpha < 1$, or a scaling decay

$$\Phi(t) \propto (t/\tau)^{-\beta} \tag{2}$$

with $0 < \beta < 1$. Here we consider the algebraic pattern (2) which is observed in the stress relaxation of viscoelastic materials, such as polymers [3–5] or critical gels [6–8], in the charge carrier transport in amorphous semiconductors [9, 10], in the behaviour of electrical currents at rough blocking electrodes [11], in dielectric relaxation [12, 13] and in the attenuation of seismic waves [14].

Even more complex behaviours are exhibited in crossover situations, typified by changes from one form of power-law decay to another. Examples can be found in the dynamics of polymers [15] and of networks [6–8] and in transient photoconductivity [9, 10]. Such crossover forms may be due to the finite extensions of the underlying systems, i.e. here to the restricted motion of polymer segments, to the fact that pre- and post-gel networks are self-similar only in restricted ranges and to the fact that photoconductive carriers move in a medium of finite thickness.

0305-4470/95/236567+18$19.50

An appropriate tool to describe phenomenologically this richness of dynamical features is fractional calculus (FC) to which a lot of theoretical work is devoted [8, 16–24]. FC was incorporated into standard constitutive equations in a variety of works, mainly in the field of viscoelasticity [3–5, 16–18]. Current models of viscoelasticity involving FC are based on the formal replacement in ordinary rheological constitutive equations (RCE) of first-order derivatives (d/dt) by fractional derivatives (d^β/dt^β) of non-integer order ($0 < \beta < 1$). However, this formal procedure cannot assure *a priori* that the resulting expressions are always physically reasonable; this aspect was pointed out for instance in references [3, 16, 19, 20].

It is therefore indispensable to have at hand a consistent procedure that automatically guarantees mechanical and thermodynamical stability. Beginning from commonly used representations of viscoelastic behaviour through mechanical models, we present here an approach which guarantees that the FC equations which follow are physically meaningful. To this end we introduce mechanical models, which in addition to purely elastic and viscous components also include fractional elements; the dynamical properties of such elements are intermediate between purely solid and purely liquid features.

We begin in the next section with a brief discussion of the way in which, as a result of the superposition principle, FC comes into play in systems governed by scaling decays. In section 3 we generalize well known prototypes of viscoelasticity (the Maxwell, the Kelvin–Voigt, the Zener and the Poynting–Thomson model) and we show that they lead to exactly solvable fractional expressions. For these we present the solutions in terms of Fox H-functions.

2. Fractional calculus: a mimicry of memory

Non-Debye relaxation implies memory. In the formal context memory can be incorporated through a causal convolution [25, 26]:

$$\sigma(t) = \int_{-\infty}^{t} dt'\, G(t-t')\frac{d\epsilon(t')}{dt'}. \tag{3}$$

The (Boltzmann) superposition integral, equation (3), holds for linear systems which are homogeneous in time; here $\sigma(t)$ denotes the stress, $\epsilon(t)$ the strain and $G(t)$ the relaxation modulus, i.e. the response of the stress to a shear jump. Consider now a system whose stress decays after a shear jump in an algebraic manner, similar to equation (2). Its stress relaxation modulus then obeys:

$$G(t) = \frac{E}{\Gamma(1-\beta)}\left(\frac{t}{\tau}\right)^{-\beta} \tag{4}$$

where E and τ are constants and $\Gamma(x)$ is the complete Gamma function. For convenience we chose the prefactors in (4) in a way which matches our forthcoming definitions. Combining equations (3) and (4) one arrives at

$$\sigma(t) = \frac{E\tau^\beta}{\Gamma(1-\beta)}\int_{-\infty}^{t} dt'\,(t-t')^{-\beta}\frac{d\epsilon(t')}{dt'}. \tag{5}$$

The right-hand side of equation (5) represents a fractional integral (FI). To see this we start from Riemann's expressions of a FI [27, 28]

$${}_cD_t^{-\gamma} f(t) = \frac{1}{\Gamma(\gamma)}\int_c^t dt'\,\frac{f(t')}{(t-t')^{1-\gamma}} \tag{6}$$

where $\gamma > 0$. Equation (6) includes two special FI forms. For $c = 0$ one recovers the Riemann–Liouville FI formulated as a Laplace convolution, whereas for $c \to -\infty$ equation (6) corresponds to Weyl's FI. For γ a positive integer, equation (6) presents a multiple (Cauchy) integral of order $-\gamma$. Now the fractional differentiation of order $\gamma > 0$ is obtained by first picking an integer n, $n > \gamma$, then performing a FI of order $\gamma - n$, followed by an ordinary differentiation of order n, i.e.

$$ {}_cD_t^{\gamma} f(t) = \frac{d^n}{dt^n}({}_cD_t^{\gamma-n} f(t)). \tag{7}$$

Working within Weyl's FI, i.e. $c \to -\infty$, we use the shorthand notation $d^{\beta}/dt^{\beta} \equiv {}_{-\infty}D_t^{\beta}$.

Using these expressions we can rewrite equation (5) as

$$\sigma(t) = E\tau^{\beta}\frac{d^{\beta-1}}{dt^{\beta-1}}\frac{d\epsilon(t)}{dt} = E\tau^{\beta}\frac{d^{\beta}\epsilon(t)}{dt^{\beta}}. \tag{8}$$

We stop to note that Weyl's formalism follows naturally from the causal convolution, equation (5), in which the strain fields start in the distant past, so that $c \to -\infty$. On the other hand restricting the dynamics to positive times only, i.e. setting $\sigma = \epsilon \equiv 0$ for $t \leqslant 0$ leads to the Riemann–Liouville formalism. This corresponds to an initial-value problem, in which the initial values must be specified [3, 21].

In the following we apply Weyl's FC and consider arbitrary histories of the system. Weyl's FC turns out to be very convenient: the composition rule for differentiations and integrations obeys the simple form

$$\frac{d^{\alpha}}{dt^{\alpha}}\frac{d^{\beta}}{dt^{\beta}} = \frac{d^{\alpha+\beta}}{dt^{\alpha+\beta}} \tag{9}$$

for arbitrary α and β [28]. Furthermore, the Fourier integration

$$\mathcal{F}\{f(t);\omega\} = \tilde{f}(\omega) = \int_{-\infty}^{\infty} dt\, f(t)\exp(-i\omega t) \tag{10}$$

transforms the operation d^{α}/dt^{α} into a simple multiplication [27, 28]:

$$\mathcal{F}\left\{\frac{d^{\alpha}f(t)}{dt^{\alpha}};\omega\right\} = (i\omega)^{\alpha}\tilde{f}(\omega). \tag{11}$$

3. Generalization of viscoelastic models

Usually phenomenologic viscoelastic models are based on springs and dashpots [25, 26], see figure 1. The springs obey Hooke's law

$$\sigma(t) = E\epsilon(t) \tag{12}$$

whereas for dashpots Trouton's (or Newton's) law holds:

$$\sigma(t) = \eta\frac{d\epsilon(t)}{dt}. \tag{13}$$

In equations (12) and (13) E and η denote the spring constant and the viscosity. Through combinations of springs and dashpots one arrives at standard viscoelastic models, such as the Maxwell or the Zener model (see later); these models involve a fairly small number of single elements [25, 26]. The problem here is that the corresponding ordinary differential equations have a relatively restricted class of solutions, which is, in general, too limited to provide an adequate description for the complex systems discussed in the introduction.

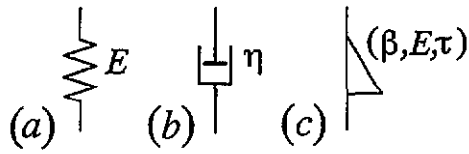

Figure 1. Single elements: (*a*) elastic, (*b*) viscous and (*c*) fractional element.

To overcome this shortcoming one can relate stress and strain through fractional equations [3–5, 8, 16–18], see equation (8). In this way one readily obtains scaling decays. In general, FC allows the interpolation between the purely elastic behaviour of equation (12), obtained for $\beta = 0$ in equation (8), and the purely viscous pattern of equation (13), obtained for $\beta = 1$ in equation (8). The interpolating RCE, equation (8) with $0 < \beta < 1$, describes for instance the behaviour of cross-linking polymers at the gel point (gel equation) [6–8].

Schiessel and Blumen [8, 20], Schiessel *et al* [29] and Heymans and Bauwens [30] have demonstrated that the fractional relation, equation (8), can be realized physically through hierarchical arrangements of springs and dashpots, such as ladders, trees or fractal structures. In the limit of an infinite number of constituting elements these arrangements obey equation (8). As an example, figure 2 presents such an arrangement; we have used it in [20]. This hierarchical structure consists of springs (with spring constants E_0, E_1, E_2, ...) along one of the struts and dashpots (with viscosities η_0, η_1, η_2, ...) on the rungs of the ladder. By adjusting the constants of the structural parts in a suitable way one can achieve for any preassigned β with $0 < \beta < 1$ that the resulting arrangement obeys equation (8) [20]. Micro- and mesoscopic interpretations of such sequential viscoelastic structures can be found in [8, 31, 32].

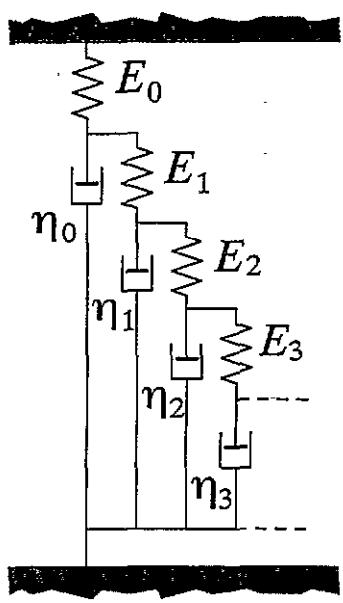

Figure 2. Sequential realization of the fractional element.

We now introduce the term *fractional element* (FE) to denote such a hierarchical structure and we symbolize it by a triangle (cf figure 1(*c*)) which schematically resembles a ladder

such as the one drawn in figure 2. Since we do not care for the specific inner details of such a hierarchical structure we specify it by the triple (β, E, τ). In the models which follow FEs are fundamental elements, besides the springs and the dashpots.

In the following we focus on mechanical models with FEs, for which we can provide solutions to all the relevant response functions [25,26], i.e. the complex modulus, the complex compliance, the relaxation modulus and the creep compliance. In this way we have closed form, analytic expressions for several observable quantities based on models which contain a limited set of parameters.

3.1. The single fractional element

We start with this simple case which sets the pattern for the analysis of the more complex models which follow. Fourier transforming equation (8) and using equation (11) results in the algebraic relation

$$\tilde{\sigma}(\omega) = E(\mathrm{i}\omega\tau)^{\beta}\tilde{\epsilon}(\omega) \tag{14}$$

from which the complex modulus

$$G^*(\omega) \equiv \tilde{\sigma}(\omega)/\tilde{\epsilon}(\omega) \tag{15}$$

can be directly recovered:

$$G^*(\omega) = E(\mathrm{i}\omega\tau)^{\beta}. \tag{16}$$

Now the relaxation modulus $G(t)$ may be obtained either from the storage modulus $G'(\omega) = \mathrm{Re}\, G^*(\omega)$ or from the loss modulus $G''(\omega) = \mathrm{Im}\, G^*(\omega)$. The relations connecting the moduli are [25]

$$G(t) = \frac{2}{\pi}\int_0^{\infty} \mathrm{d}\omega\, \frac{G'(\omega)}{\omega}\sin\omega t = \mathcal{F}_{\mathrm{S}}^{-1}\left\{\frac{G'(\omega)}{\omega}; t\right\} \tag{17}$$

and

$$G(t) = \frac{2}{\pi}\int_0^{\infty} \mathrm{d}\omega\, \frac{G''(\omega)}{\omega}\cos\omega t = \mathcal{F}_{\mathrm{C}}^{-1}\left\{\frac{G''(\omega)}{\omega}; t\right\}. \tag{18}$$

In equations (17) and (18), $\mathcal{F}_{\mathrm{S}}^{-1}$ and $\mathcal{F}_{\mathrm{C}}^{-1}$ denote the inverse Fourier sine and cosine transformations; the direct transformations are $\mathcal{F}_{\mathrm{S}}\{f(t);\omega\} = \int_0^{\infty}\mathrm{d}t f(t)\sin\omega t$ and $\mathcal{F}_{\mathrm{C}}\{f(t);\omega\} = \int_0^{\infty}\mathrm{d}t\, f(t)\cos\omega t$. For a single FE one obtains readily from (17)

$$G(t) = \mathcal{F}_{\mathrm{S}}^{-1}\left\{E\tau^{\beta}\cos\left(\frac{\pi\beta}{2}\right)\omega^{\beta-1}; t\right\} = \frac{E}{\Gamma(1-\beta)}\left(\frac{t}{\tau}\right)^{-\beta}. \tag{19}$$

Here equation (3.768(1.)) of [33] was used for establishing the second equality on the right-hand side. This result reproduces equation (4).

On the other hand, the complex compliance obeys $J^*(\omega) = 1/G^*(\omega)$, so that here $J^*(\omega) = E^{-1}(\mathrm{i}\omega\tau)^{-\beta}$. Again, the storage and loss compliances are given by $J'(\omega) = \mathrm{Re}\, J^*(\omega)$ and by $J''(\omega) = -\mathrm{Im}\, J^*(\omega)$, respectively. These compliances are related to the creep compliance $J(t)$ (i.e. the response of the strain to a stress jump $\sigma(t) = \Theta(t)$) through [25]:

$$\frac{\mathrm{d}J(t)}{\mathrm{d}t} = \mathcal{F}_{\mathrm{C}}^{-1}\{J'(\omega); t\} = -\mathcal{F}_{\mathrm{S}}^{-1}\{J''(\omega); t\}. \tag{20}$$

Hence we obtain for the FE

$$\frac{\mathrm{d}J(t)}{\mathrm{d}t} = \mathcal{F}_{\mathrm{C}}^{-1}\left\{E^{-1}\tau^{-\beta}\cos\left(\frac{\pi\beta}{2}\right)\omega^{-\beta}; t\right\} = \frac{E^{-1}\tau^{-\beta}}{\Gamma(\beta)}t^{\beta-1} \tag{21}$$

where we used equation (3.768(2.)) from [33]. From equation (21) we obtain $J(t)$ by integration (using $J(0) = 1/G(0) = 0$ [25]):

$$J(t) = \frac{E^{-1}}{\Gamma(1+\beta)} \left(\frac{t}{\tau}\right)^{\beta}. \tag{22}$$

3.2. The generalized Maxwell model

Figure 3(a) shows the standard Maxwell model in which a spring and a dashpot are arranged in series [25, 26]. We generalize this model by replacing these elements by the FEs (α, E_1, τ_1) and (β, E_2, τ_2), see figure 3(b). Because of the sequential construction $\sigma(t)$ is the same for both elements. Their respective stress–strain relations are

$$\epsilon_1(t) = E_1^{-1}\tau_1^{-\alpha}\frac{\mathrm{d}^{-\alpha}\sigma(t)}{\mathrm{d}t^{-\alpha}} \tag{23}$$

and

$$\epsilon_2(t) = E_2^{-1}\tau_2^{-\beta}\frac{\mathrm{d}^{-\beta}\sigma(t)}{\mathrm{d}t^{-\beta}} \tag{24}$$

where both expressions follow from the composition rule (9). Due to the construction of the generalized Maxwell model, we have $\epsilon(t) = \epsilon_1(t) + \epsilon_2(t)$, from which it follows

$$\sigma(t) + \frac{E_1\tau_1^{\alpha}}{E_2\tau_2^{\beta}}\frac{\mathrm{d}^{\alpha-\beta}\sigma(t)}{\mathrm{d}t^{\alpha-\beta}} = E_1\tau_1^{\alpha}\frac{\mathrm{d}^{\alpha}\epsilon(t)}{\mathrm{d}t^{\alpha}}. \tag{25}$$

In equation (25) we assumed $\alpha \geqslant \beta$ without loss of generality. For $\alpha = \beta$ we recover basically the RCE of the single FE, as discussed in subsection 3.1. We now take $\alpha > \beta$. Equation (25) can be simplified by setting $\tau = (E_1\tau_1^{\alpha}/E_2\tau_2^{\beta})^{1/(\alpha-\beta)}$ and $E = E_1(\tau_1/\tau)^{\alpha}$. This leads to

$$\sigma(t) + \tau^{\alpha-\beta}\frac{\mathrm{d}^{\alpha-\beta}\sigma(t)}{\mathrm{d}t^{\alpha-\beta}} = E\tau^{\alpha}\frac{\mathrm{d}^{\alpha}\epsilon(t)}{\mathrm{d}t^{\alpha}} \tag{26}$$

which is the RCE of the generalized Maxwell model [16, 34].

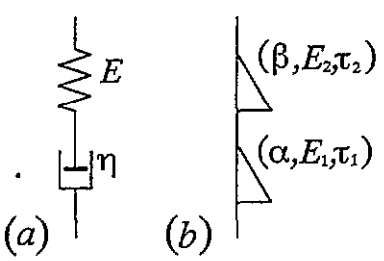

Figure 3. The Maxwell element (a) and its fractional generalization (b).

Fourier transforming equation (26) and using equations (11) and (15) leads to the complex modulus

$$G^*(\omega) = \frac{E(\mathrm{i}\omega\tau)^{\alpha}}{1 + (\mathrm{i}\omega\tau)^{\alpha-\beta}}. \tag{27}$$

In order to calculate the relaxation modulus $G(t)$ we use the loss modulus $G''(\omega) = \mathrm{Im}\, G^*(\omega)$. Hence, from (27):

$$G''(\omega) = E\frac{(\omega\tau)^{\alpha}\sin(\pi\alpha/2) + (\omega\tau)^{2\alpha-\beta}(\sin\pi\beta/2)}{1 + (\omega\tau)^{2(\alpha-\beta)} + 2(\omega\tau)^{\alpha-\beta}\cos(\pi(\alpha-\beta)/2)}. \tag{28}$$

Now following equation (18) and the results of the appendix we find for the Mellin transform of $G''(\omega)/\omega$ after some tedious calculations

$$\mathcal{M}\left\{\frac{G''(\omega)}{\omega};z\right\} = \frac{\pi E}{\alpha-\beta}\frac{\cos(\pi z/2)}{\sin(\pi(z+\alpha-1)/(\alpha-\beta))}\tau^{1-z} \tag{29}$$

where equation (2.54) of [35] was used. In equation (29) the Mellin transform $\mathcal{M}$ is defined by

$$\hat{f}(z) \equiv \mathcal{M}\{f(x);z\} = \int_0^\infty \mathrm{d}x\, f(x)x^{z-1} \tag{30}$$

which is also known as the double-sided Laplace transform [35–37]. The relation between $\mathcal{M}\{G''(\omega)/\omega\}$ and $\mathcal{M}\{G(t)\}$ is given by

$$\mathcal{M}\left\{\frac{G''(\omega)}{\omega};z\right\} = \Gamma(z)\cos\left(\frac{\pi z}{2}\right)\mathcal{M}\{G(t);1-z\} \tag{31}$$

(cf equations (18) and (A2)). From equations (29) and (31) we obtain $G(t)$ via an inverse Mellin transform (cf (A3)):

$$\begin{aligned} G(t) &= \frac{E}{\alpha-\beta}\mathcal{M}^{-1}\left\{\frac{\Gamma\left(\frac{\alpha-z}{\alpha-\beta}\right)\Gamma\left(\frac{-\beta+z}{\alpha-\beta}\right)}{\Gamma(1-z)}\tau^z;t\right\} \\ &= \frac{E}{\alpha-\beta}H_{12}^{11}\left[\frac{t}{\tau}\middle|\begin{matrix}\left(\frac{-\beta}{\alpha-\beta},\frac{1}{\alpha-\beta}\right)\\ \left(\frac{-\beta}{\alpha-\beta},\frac{1}{\alpha-\beta}\right)\end{matrix};(0,1)\right]. \end{aligned} \tag{32}$$

Here we used the connection between the inverse Mellin transform and the definition integral of the Fox H-function [38], see the appendix, equations (A3) and (A4). By further use of the properties of the H-function we can rewrite equation (32) in terms of Maitland's generalized hypergeometric function ${}_1\Psi_1(t/\tau)$ [38], or as the better known generalized Mittag–Leffler function [36]

$$G(t) = E\left(\frac{t}{\tau}\right)^{-\beta}E_{\alpha-\beta,1-\beta}\left(-\left(\frac{t}{\tau}\right)^{\alpha-\beta}\right) \tag{33}$$

valid for arbitrary $0 \leqslant \beta < \alpha \leqslant 1$. The equivalence between equations (32) and (33) can be seen by comparing the power series expansion of the H-function, equation (A10), with the definition of the generalized Mittag–Leffler function [36]:

$$E_{\kappa,\mu}(x) = \sum_{n=0}^{\infty}\frac{x^n}{\Gamma(\kappa n+\mu)}. \tag{34}$$

The main result, equations (32) and (33), was also derived by Glöckle and Nonnenmacher [3] via a similar approach involving the Laplace–Mellin technique and by Friedrich [16] using a power series ansatz. In the parameter range $0 \leqslant \beta < \alpha < 1$, $G(t)$ obeys at short times, $t \ll \tau$ (cf (A13)),

$$G(t) \cong \frac{E}{\Gamma(1-\beta)}\left(\frac{t}{\tau}\right)^{-\beta} \tag{35}$$

whereas at long times ($t \gg \tau$) one has asymptotically (cf (A14))

$$G(t) \cong \frac{E}{\Gamma(1-\alpha)}\left(\frac{t}{\tau}\right)^{-\alpha}. \tag{36}$$

Expressions (32) and (33) also embrace the special cases $\beta = 0$ and $\alpha = 1$. For $\beta = 0$ and arbitrary $0 < \alpha \leqslant 1$, one has $G(t) = EE_\alpha(-(t/\tau)^\alpha)$, a result which was also found in [16, 18]. Here E_α is the standard Mittag–Leffler function $E_\alpha(x) = E_{\alpha,1}(x)$ [36]. For $\alpha = 1$, E_α turns into a simple exponential (cf equation (34) with $\kappa = \mu = 1$) and hence $G(t) = E\exp(-t/\tau)$, this being the exponential decaying response of the standard Maxwell model (i.e. $\beta = 0$ and $\alpha = 1$). Finally for $\alpha = 1$ and β in the range $]0, 1[$ the relaxation modulus, equation (32), shows the following behaviour at long times, $t \gg \tau$:

$$G(t) \cong \frac{-E}{\Gamma(\beta - 1)} \left(\frac{t}{\tau}\right)^{\beta-2} \tag{37}$$

whereas the short-time behaviour is still given by equation (35). This can be seen from the expansion of the H-function for small and large values, equations (A10) and (A12). Note that for $\alpha = 1$ the first term of the power series on the right-hand side of equation (A12) vanishes due to the occurrence of a pole of the Γ-function; thus the long-time decay is governed by the second term. Compared to the long-time decay in the case $\alpha < 1$, equation (36), we have here a faster relaxation for $t \gg \tau$. In our picture of mechanical analogues the case $\alpha = 1$ corresponds to a simple dashpot. This purely viscous element causes a faster decay so that one has a fluid long-time behaviour [16]: when one deforms the system continuously (e.g. $\epsilon(t) = vt$) the stress $\sigma(t)$ remains finite for all times (cf the superposition integral, equation(3)).

Using the power series (A10) and (A12) the relaxation modulus $G(t)$ of the fractional Maxwell model can be also evaluated numerically. The result is displayed in figure 4 for two different sets of parameters together with the exponential decaying response of the ordinary Maxwell model. The asymptotic short- and long-time regimes of the fractional models show clearly the algebraic patterns given in equations (35) and (36).

At this stage it is worth mentioning that physical constraints are automatically fulfilled by our generalized Maxwell model; this is, of course a direct consequence of our derivation of the RCE (26) from mechanical analogues. In equation (26) this is manifested in the fact that the order of the fractional derivative on the stress, $\alpha - \beta$, is always less or equal than that operating on the strain, α. This is an important requirement for thermodynamic stability [3, 16]. It is obvious that such conditions are not automatically fulfilled by simply replacing integer-order by fractional-order operators. Furthermore, if one now also requires that $G(t)$ stays finite for $t \to 0$ (as befits a well-defined initial-value problem) we must require that $\beta = 0$, see equation (35) and [34]. Physically $\beta = 0$ corresponds to a simple spring, which is able to deform instantaneously (i.e. to perform a stress jump), so that $G(0) = E$, see equation (35).

The complex compliance $J^*(\omega) = 1/G^*(\omega)$ follows from equation (27)

$$J^*(\omega) = E^{-1}(\mathrm{i}\omega\tau)^{-\alpha} + E^{-1}(\mathrm{i}\omega\tau)^{-\beta}. \tag{38}$$

This mirrors the fact that for serially-arranged elements the compliances simply add. Using the same steps which led from equation (20) to equation (22) we have

$$J(t) = E^{-1}\frac{(t/\tau)^\alpha}{\Gamma(1+\alpha)} + E^{-1}\frac{(t/\tau)^\beta}{\Gamma(1+\beta)} \tag{39}$$

for all $0 \leqslant \beta \leqslant \alpha \leqslant 1$, a result also reported in [16] (see also the discussion in [3]).

3.3. The generalized Kelvin–Voigt model

When one arranges the spring and the dashpot in parallel one arrives at the standard Kelvin–Voigt model, shown in figure 5(*a*). Its generalization with two FEs is depicted in figure 5(*b*).

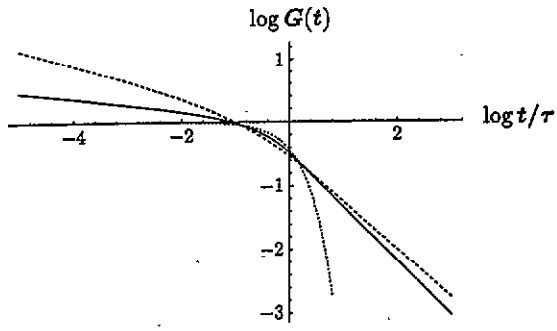

Figure 4. The relaxation modulus of the generalized Maxwell model with the parameters (α, β) chosen as (0.85, 0.1), (0.75, 0.25) (dashed curve) and the standard case (1, 0) (dotted curve). In all cases we set $E = 1$.

Because of the construction the individual stresses add. Following the procedure used in the previous subsection we have as corresponding RCE

$$\sigma(t) = E\tau^{\alpha}\frac{\mathrm{d}^{\alpha}\epsilon(t)}{\mathrm{d}t^{\alpha}} + E\tau^{\beta}\frac{\mathrm{d}^{\beta}\epsilon(t)}{\mathrm{d}t^{\beta}} \tag{40}$$

where we have introduced the parameters $\tau = (E_1\tau_1^{\alpha}/E_2\tau_2^{\beta})^{1/(\alpha-\beta)}$ and $E = E_1(\tau_1/\tau)^{\alpha}$. By Fourier transforming equation (40) we obtain from equations (11) and (15) the complex modulus

$$G^*(\omega) = E(\mathrm{i}\omega\tau)^{\alpha} + E(\mathrm{i}\omega\tau)^{\beta} \tag{41}$$

a result that mirrors the additivity of the moduli in parallel arrangements. Repeating the steps from equation (16) to equation (19) we get

$$G(t) = E\frac{(t/\tau)^{-\alpha}}{\Gamma(1-\alpha)} + E\frac{(t/\tau)^{-\beta}}{\Gamma(1-\beta)}. \tag{42}$$

On the other hand, here in the Kelvin–Voigt model, the parallel arrangement causes the complex compliance

$$J^*(\omega) = E^{-1}\frac{(\mathrm{i}\omega\tau)^{-\beta}}{1+(\mathrm{i}\omega\tau)^{\alpha-\beta}} \tag{43}$$

to be more involved than in the Maxwell model. For the calculation of the function $J(t)$ one can follow a way analogous to the evaluation of $G(t)$ in the preceding subsection. One can start from the real part of $J^*(\omega)$, the storage compliance

$$J'(\omega) = E^{-1}\frac{(\omega\tau)^{-\beta}\cos(\pi\beta/2) + (\omega\tau)^{\alpha-2\beta}\cos(\pi\alpha/2)}{1+(\omega\tau)^{2(\alpha-\beta)} + 2(\omega\tau)^{\alpha-\beta}\cos(\pi(\alpha-\beta)/2)} \tag{44}$$

which has to be transformed according to equation (20). Note the structural symmetry to $G''(\omega)$ of the Maxwell model, equation (28). This simplifies the procedure, and using the Fourier–Mellin technique as before, we obtain

$$\frac{\mathrm{d}J(t)}{\mathrm{d}t} = \frac{(E\tau)^{-1}}{\alpha-\beta}H_{12}^{11}\left[\frac{t}{\tau}\,\middle|\,\begin{matrix}\left(\frac{\alpha-1}{\alpha-\beta},\frac{1}{\alpha-\beta}\right)\\ \left(\frac{\alpha-1}{\alpha-\beta},\frac{1}{\alpha-\beta}\right)\end{matrix};(0,1)\right]. \tag{45}$$

By integration, using equation (A11) together with $J(0) = 1/G(0) = 0$, we obtain

$$J(t) = \frac{E^{-1}}{\alpha-\beta} H_{12}^{11}\left[\frac{t}{\tau}\middle|\begin{matrix}\left(\frac{\alpha}{\alpha-\beta},\frac{1}{\alpha-\beta}\right)\\ \left(\frac{\alpha}{\alpha-\beta},\frac{1}{\alpha-\beta}\right)\end{matrix}; (0,1)\right]$$
$$= E^{-1}\left(\frac{t}{\tau}\right)^{\alpha} E_{\alpha-\beta,1+\alpha}\left(-\left(\frac{t}{\tau}\right)^{\alpha-\beta}\right). \tag{46}$$

Here we give on the right-hand side of (46) also the corresponding generalized Mittag–Leffler function. The result is valid for all $0 \leqslant \beta < \alpha \leqslant 1$. To our best knowledge, equation (46) for $J(t)$ has not been presented before in the literature on relaxation in complex media. From equation (A13) we obtain the short time behaviour, $t \ll \tau$, of $J(t)$:

$$J(t) \cong \frac{E^{-1}}{\Gamma(1+\alpha)}\left(\frac{t}{\tau}\right)^{\alpha} \tag{47}$$

whereas for $t \gg \tau$ we obtain asymptotically (cf (A14))

$$J(t) \cong \frac{E^{-1}}{\Gamma(1+\beta)}\left(\frac{t}{\tau}\right)^{\beta}. \tag{48}$$

We stop to note that these expressions also hold for $\alpha = 1$. One should notice the similarity of equations (47) and (48) to the corresponding expressions (35) and (36) of the Maxwell model.

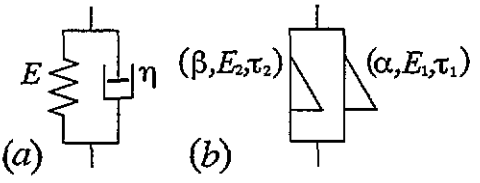

Figure 5. The (*a*) ordinary and (*b*) fractional Kelvin–Voigt element.

For $\beta = 0$ and arbitrary $0 < \alpha \leqslant 1$, $J(t)$ given by (46) may be expressed in terms of the standard Mittag–Leffler function (cf equation (18.1.23) of [36])

$$J(t) = E^{-1} - E^{-1}E_{\alpha}\left(-\left(\frac{t}{\tau}\right)^{\alpha}\right) \tag{49}$$

a result which was already given by Gross [39] (see also [18]). For $\alpha = 1$ one has $J(t) = E^{-1} - E^{-1}\exp(-t/\tau)$, i.e. the well known exponential behaviour of the standard Kelvin–Voigt model. Finally, for $\alpha = 1$ and $0 < \beta < 1$ the result

$$J(t) = E^{-1}\frac{(t/\tau)^{\beta}}{\Gamma(1+\beta)} - E^{-1}\left(\frac{t}{\tau}\right)^{\beta} E_{1-\beta,1+\beta}\left(-\left(\frac{t}{\tau}\right)^{1-\beta}\right) \tag{50}$$

is obtained from equation (46). Note that for $t \to \infty$, J stays finite only when $\beta = 0$, i.e. when in the Kelvin–Voigt arrangement there is a spring in parallel.

Here we note the symmetry of the dynamical response functions, $G(t)$ and $J(t)$, in the two possible arrangements of two FEs, namely in the generalized Maxwell model and in the generalized Kelvin–Voigt model. Depending on the sequential (Maxwell) or parallel (Kelvin–Voigt) construction one of these response functions is simply a sum of two algebraic terms (i.e. $J(t)$ in the Maxwell model, equation (39), and $G(t)$ in the Kelvin–Voigt model, equation (42)). Then the other response function is a Mittag–Leffler function (i.e. $G(t)$ for

the Maxwell model, equation (33), and $J(t)$ for the Kelvin–Voigt model, equation (46)). Moreover, in every case one witnesses a crossover between two algebraic regimes: for a sum of two algebraic terms this is obvious; in the case of the Mittag–Leffler function this follows from its expression through power series (see above and equations (A13) and (A14)).

3.4. The generalized Zener model

The so-called Zener or standard solid model [25,26] involves three elements as shown in figure 6(*a*). It consists of a Maxwell model in parallel with a spring. The most general fractional version of the Zener model is displayed in figure 6(*b*) and consists of three FEs. Without loss of generality, we again require $0 \leqslant \beta < \alpha \leqslant 1$ and, of course, $0 \leqslant \gamma \leqslant 1$. Then the stresses in the left, $\sigma_L(t)$, and right, $\sigma_R(t)$, branches of the model are given by

$$\sigma_L(t) + \tau_0^{\alpha-\beta}\frac{d^{\alpha-\beta}\sigma_L(t)}{dt^{\alpha-\beta}} = E_0\tau_0^{\alpha}\frac{d^{\alpha}\epsilon(t)}{dt^{\alpha}} \tag{51}$$

and

$$\sigma_R(t) = E_3\tau_3^{\gamma}\frac{d^{\gamma}\epsilon(t)}{dt^{\gamma}}. \tag{52}$$

In equation (51) we set $\tau_0 = (E_1\tau_1^{\alpha}/E_2\tau_2^{\beta})^{1/(\alpha-\beta)}$ and $E_0 = E_1(\tau_1/\tau_0)^{\alpha}$. Both stresses add up to the RCE

$$\sigma(t) + \tau_0^{\alpha-\beta}\frac{d^{\alpha-\beta}\sigma(t)}{dt^{\alpha-\beta}} = E_0\tau_0^{\alpha}\frac{d^{\alpha}\epsilon(t)}{dt^{\alpha}} + E_3\tau_3^{\gamma}\frac{d^{\gamma}\epsilon(t)}{dt^{\gamma}} + E_3\tau_3^{\gamma}\tau_0^{\alpha-\beta}\frac{d^{\gamma+\alpha-\beta}\epsilon(t)}{dt^{\gamma+\alpha-\beta}}. \tag{53}$$

Setting now $\tau = \tau_0$ and $E = E_3(\tau_3/\tau)^{\gamma}$, equation (53) reads

$$\sigma(t) + \tau^{\alpha-\beta}\frac{d^{\alpha-\beta}\sigma(t)}{dt^{\alpha-\beta}} = E_0\tau^{\alpha}\frac{d^{\alpha}\epsilon(t)}{dt^{\alpha}} + E\tau^{\gamma}\frac{d^{\gamma}\epsilon(t)}{dt^{\gamma}} + E\tau^{\gamma+\alpha-\beta}\frac{d^{\gamma+\alpha-\beta}\epsilon(t)}{dt^{\gamma+\alpha-\beta}}. \tag{54}$$

This RCE was given by Tschoegl [26] for the special case $\beta = \gamma = 0$. It was extended to arbitrary $0 \leqslant \beta < \alpha$ (with $\gamma = 0$) by Friedrich and Braun [5], where also a comparison of this model with experimental results for different polymer systems (polymeric glasses and gelling systems) can be found.

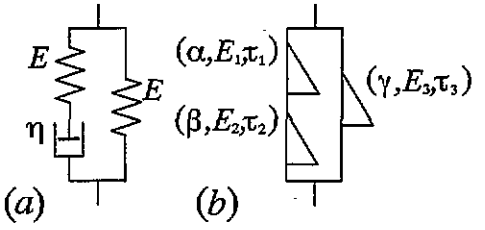

Figure 6. The Zener model (*a*) and its fractional generalization (*b*).

Using equations (11) and (15) the calculation of the complex modulus $G^*(\omega)$ is straightforward and results in

$$G^*(\omega) = \frac{E_0(i\omega\tau)^{\alpha} + E(i\omega\tau)^{\gamma} + E(i\omega\tau)^{\gamma+\alpha-\beta}}{1 + (i\omega\tau)^{\alpha-\beta}} = E_0\frac{(i\omega\tau)^{\alpha}}{1 + (i\omega\tau)^{\alpha-\beta}} + E(i\omega\tau)^{\gamma}. \tag{55}$$

In equation (55) the moduli of the Maxwell model and of a single FE add; this is the direct consequence of the parallel arrangement of figure 6(*b*).

We obtain the resulting relaxation modulus from equation (55) by simply adding the moduli of the Maxwell model, equation (32), and of the single FE, equation (19), i.e.

$$G(t) = \frac{E_0}{\alpha-\beta} H_{12}^{11}\left[\frac{t}{\tau}\middle|\begin{matrix}\left(-\frac{\beta}{\alpha-\beta},\frac{1}{\alpha-\beta}\right)\\ \left(-\frac{\beta}{\alpha-\beta},\frac{1}{\alpha-\beta}\right)\end{matrix}; (0,1)\right] + E\frac{(t/\tau)^{-\gamma}}{\Gamma(1-\gamma)}. \tag{56}$$

Depending on the parameters up to four time regimes with algebraic behaviours may occur. This can be seen by comparing on the right-hand side of equation (56) the generalized Maxwell term (and its power-law behaviours, equations (35) and (36)) with the second term. For instance, for the case $\gamma \leqslant \beta$ and for $((E_0/E)(\Gamma(1-\gamma)/\Gamma(1-\alpha)))^{1/(\alpha-\gamma)} \gg 1$, we find three time regimes

$$G(t) \sim \begin{cases} t^{-\beta} & \text{for } t \ll \tau \\ t^{-\alpha} & \text{for } \tau \ll t \ll \tau_1 \\ t^{-\gamma} & \text{for } \tau_1 \ll t \end{cases} \tag{57}$$

where $\tau_1 = ((E_0/E)(\Gamma(1-\gamma)/\Gamma(1-\alpha)))^{1/(\alpha-\gamma)}\tau$. In addition to the three regimes of equation (57), one has in the case $\alpha > \gamma > \beta$ also a fourth regime $G(t) \sim t^{-\gamma}$ at very short times, $t \ll \tau_2$ where $\tau_2 = ((E/E_0)(\Gamma(1-\beta)/\Gamma(1-\gamma)))^{1/(\gamma-\beta)}\tau$.

Note that for special values of the parameters, $G(t)$ follows from the results of the single FE and of the Maxwell models, as discussed in subsections 3.1 and 3.2. Note especially that the case $\alpha = 1$, $\beta = \gamma = 0$ reduces to the exponentially decreasing relaxation function of the standard Zener model [26].

Using the power series (A10) and (A12) we have evaluated numerically $G(t)$ for the fractional Zener model. The result is shown in figure 7 for three different sets of parameters. The three power-law regimes of equation (57) can be seen clearly.

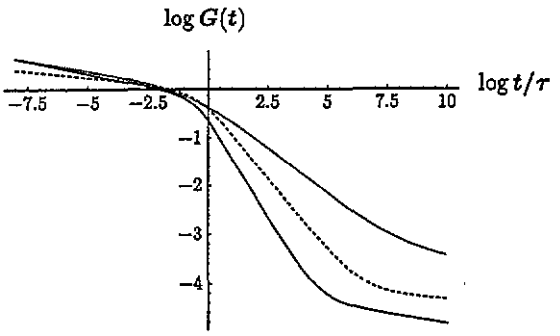

Figure 7. The relaxation modulus of the fractional Zener model with the parameters (α, β, γ) chosen as (0.8, 0.1, 0.08), (0.6, 0.05, 0.03) (dashed curve) and (0.4, 0.08, 0.05) (dotted curve). In all cases we set $E_0 = 1$ and $E = 0.0001$.

The complex compliance $J^*(\omega) = 1/G^*(\omega)$, i.e.

$$J^*(\omega) = \frac{(i\omega\tau)^{-\alpha} + (i\omega\tau)^{-\beta}}{E_0 + E(i\omega\tau)^{\gamma-\alpha} + E(i\omega\tau)^{\gamma-\beta}} \tag{58}$$

shows a more involved pattern. Within the framework of the Fourier–Mellin technique we are able to express $J(t)$ analytically for $\gamma = \alpha$ or for $\gamma = \beta$. We start by presenting the

results for the generalized Zener model with $\gamma = \alpha$:

$$J(t) = \frac{A^{(2\alpha-\beta/\alpha-\beta)}}{\alpha-\beta}\frac{E_0}{E^2}H_{12}^{11}\left[A^{-1/(\alpha-\beta)}\frac{t}{\tau}\middle|\begin{matrix}\left(\frac{\alpha}{\alpha-\beta},\frac{1}{\alpha-\beta}\right)\\ \left(\frac{\alpha}{\alpha-\beta},\frac{1}{\alpha-\beta}\right)\end{matrix};(0,1)\right] + \frac{(E_0+E)^{-1}}{\Gamma(1+\alpha)}\left(\frac{t}{\tau}\right)^{\alpha} \tag{59}$$

and with $\gamma = \beta$:

$$J(t) = \frac{A^{(\alpha-2\beta)/(\alpha-\beta)}}{\alpha-\beta}\frac{E_0}{E^2}H_{12}^{11}\left[A^{1/(\alpha-\beta)}\frac{t}{\tau}\middle|\begin{matrix}\left(\frac{\alpha}{\alpha-\beta},\frac{1}{\alpha-\beta}\right)\\ \left(\frac{\alpha}{\alpha-\beta},\frac{1}{\alpha-\beta}\right)\end{matrix};(0,1)\right] + \frac{(E_0+E)^{-1}}{\Gamma(1+\beta)}\left(\frac{t}{\tau}\right)^{\beta}. \tag{60}$$

In both cases we set $A = E/(E+E_0)$. Equation (60) was given in [5, 18] for the special case $\gamma = \beta = 0$. Note that in equations (59) and (60) $J(t)$ is simply the sum of the compliances of the Kelvin–Voigt model (cf (46)) and of the single FE, equation (22). A different version of a fractional Zener model was given in [3].

Where the derivation of equations (59) and (60) is concerned, the RCE of the Zener model has the same form as the RCE of the generalized Poynting–Thomson model which we discuss later. This duality is remarkable. Due to the serial structure of the Poynting–Thomson arrangement, its creep compliance $J(t)$ is readily obtained as the sum of the $J(t)$ of its subunits. The derivation of $J(t)$ being simpler for the Poynting–Thomson model, we restrain ourselves from presenting here the details of the more involved Fourier–Mellin technique and use in the next section the duality for a simpler derivation of equations (59) and (60).

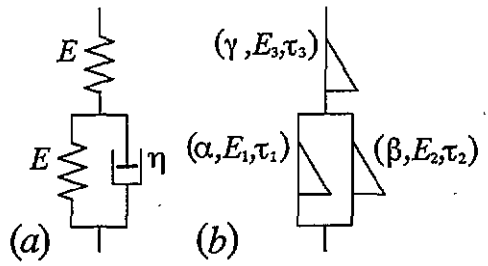

Figure 8. The (*a*) ordinary and (*b*) fractional Poynting–Thomson model.

3.5. The generalized Poynting–Thomson model

The Poynting–Thomson model and its generalization using FEs are shown in figures 8(*a*) and (*b*), respectively. The stress–strain relation of the generalized model obeys

$$\sigma(t) + \frac{E_0}{E}\tau^{\alpha-\gamma}\frac{\mathrm{d}^{\alpha-\gamma}\sigma(t)}{\mathrm{d}t^{\alpha-\gamma}} + \frac{E_0}{E}\tau^{\beta-\gamma}\frac{\mathrm{d}^{\beta-\gamma}\sigma(t)}{\mathrm{d}t^{\beta-\gamma}} = E_0\tau^{\alpha}\frac{\mathrm{d}^{\alpha}\epsilon(t)}{\mathrm{d}t^{\alpha}} + E_0\tau^{\beta}\frac{\mathrm{d}^{\beta}\epsilon(t)}{\mathrm{d}t^{\beta}} \tag{61}$$

with $\tau = (E_1\tau_1^{\alpha}/E_2\tau_2^{\beta})^{1/(\alpha-\beta)}$, $E_0 = E_1(\tau_1/\tau)^{\alpha}$ and $E = E_3(\tau_3/\tau)^{\gamma}$. Due to the serial arrangement of the Poynting–Thomson model we obtain immediately its creep compliance

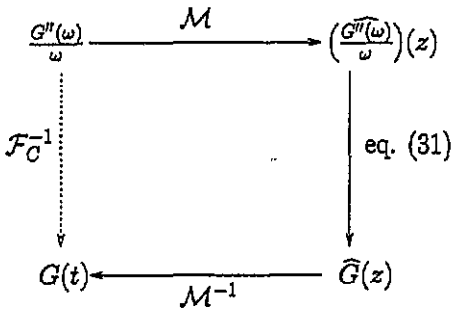

Figure 9. The inverse cosine transform for $G(t)$ and its description via a three-step procedure involving the Mellin transform and its inverse.

as the sum of the compliances of its subunits, a Kelvin–Voigt element (cf (43)) and a FE (cf (22)):

$$J(t) = \frac{E_0^{-1}}{\alpha-\beta} H_{12}^{11}\left[\frac{t}{\tau}\middle|\begin{matrix}\left(\frac{\alpha}{\alpha-\beta},\frac{1}{\alpha-\beta}\right)\\ \left(\frac{\alpha}{\alpha-\beta},\frac{1}{\alpha-\beta}\right)\end{matrix}; (0,1)\right] + \frac{E^{-1}}{\Gamma(1+\gamma)}\left(\frac{t}{\tau}\right)^{\gamma}. \tag{62}$$

We are able to calculate the relaxation modulus when we restrict ourselves to $\gamma = \alpha$ or to $\gamma = \beta$. Interestingly, the Poynting–Thomson and the Zener model lead then to the same RCEs. Thus for $\gamma = \alpha$ the RCE of the Poynting–Thomson model, equation (61), takes the form

$$\sigma(t) + \frac{E_0^{\mathrm{PT}} + E^{\mathrm{PT}}}{E_0^{\mathrm{PT}}}(\tau^{\mathrm{PT}})^{\alpha-\beta}\frac{\mathrm{d}^{\alpha-\beta}\sigma(t)}{\mathrm{d}t^{\alpha-\beta}} = E^{\mathrm{PT}}(\tau^{\mathrm{PT}})^{\alpha}\frac{\mathrm{d}^{\alpha}\epsilon(t)}{\mathrm{d}t^{\alpha}} + E^{\mathrm{PT}}(\tau^{\mathrm{PT}})^{2\alpha-\beta}\frac{\mathrm{d}^{2\alpha-\beta}\epsilon(t)}{\mathrm{d}t^{2\alpha-\beta}} \tag{63}$$

whereas the RCE of the Zener model, equation (54), for $\gamma = \alpha$ reads

$$\sigma(t) + (\tau^{\mathrm{Z}})^{\alpha-\beta}\frac{\mathrm{d}^{\alpha-\beta}\sigma(t)}{\mathrm{d}t^{\alpha-\beta}} = (E_0^{\mathrm{Z}} + E^{\mathrm{Z}})(\tau^{\mathrm{Z}})^{\alpha}\frac{\mathrm{d}^{\alpha}\epsilon(t)}{\mathrm{d}t^{\alpha}} + E^{\mathrm{Z}}(\tau^{\mathrm{Z}})^{2\alpha-\beta}\frac{\mathrm{d}^{2\alpha-\beta}\epsilon(t)}{\mathrm{d}t^{2\alpha-\beta}}. \tag{64}$$

In order to distinguish between the material constants of the two models we have introduced in equations (63) and (64) the superscripts PT for Poynting–Thomson and Z for Zener, respectively. By comparing the corresponding terms of equations (63) and (64) we find as transformation rules

$$\tau^{\mathrm{PT}} = (E^{\mathrm{Z}}/(E_0^{\mathrm{Z}} + E^{\mathrm{Z}}))^{1/(\alpha-\beta)}\tau^{\mathrm{Z}} \tag{65a}$$

$$E^{\mathrm{PT}} = (E^{\mathrm{Z}}/(E_0^{\mathrm{Z}} + E^{\mathrm{Z}}))^{(\beta-2\alpha)/(\alpha-\beta)}E^{\mathrm{Z}} \tag{65b}$$

and

$$E_0^{\mathrm{PT}} = (E^{\mathrm{Z}}/(E_0^{\mathrm{Z}} + E^{\mathrm{Z}}))^{(\beta-2\alpha)/(\alpha-\beta)}(E^{\mathrm{Z}})^2/E_0^{\mathrm{Z}}. \tag{65c}$$

Equations (65) connect the two models and are valid for $\gamma = \alpha$; for $\gamma = \beta$ one has simply to exchange α and β in (65). Using equations (62) and (65) one recovers equations (59) and (60) of the fractional Zener model.

Duality can now be invoked again to establish the relaxation modulus $G(t)$ in the Poynting–Thomson model; one has only to replace the material constants in the corresponding function of the fractional Zener model, equation (56). The discussion of $G(t)$ runs along the same lines as in the generalized Zener model, so that we do not repeat it here.

3.6. Other models

Similarly to the models discussed above, one can derive the RCE of any arrangement of elementary mechanical parts, such as springs, dashpots and FEs. From the RCE using the behaviour of the Weyl derivative under Fourier transforms, equation (11), one obtains analytically the harmonic response functions $G^*(\omega)$ and $J^*(\omega)$. Their inversion, to obtain $G(t)$ and $J(t)$ is, however, a hard task, which is not always feasible in the framework of the Fourier–Mellin technique. Nevertheless, whenever a system is built as a parallel (serial) arrangement of subunits with known relaxation moduli (creep compliances), its corresponding response function is the sum of the responses of the subunits. Using such sub-blocks a great variety of complicated systems with analytical response functions can be constructed.

4. Conclusion

In this work we have put forward a method which allows a physically correct generalization of viscoelastic models. We arrive at arrangements which obey fractional RCEs by replacing in the usual mechanical models some of the elastic and viscous elements by fractional ones. We also surveyed exactly solvable models and calculated explicitly their response functions.

The representation of generalized viscoelastic models by fractional analogues also allows a deeper insight into the physics behind fractional stress–strain relations; on the other hand RCEs aid in discovering hidden symmetries between the models, such as the duality between the fractional Zener and Poynting–Thomson models. Using fractional elements one can tailor viscoelastic models with given properties, while keeping the number of the parameters involved relatively low.

Acknowledgments

Financial support by the Deutsche Forschungsgemeinschaft (through the SFB 60 and the SFB 239), by the Fonds der Chemischen Industrie and by the PROCOPE-Programme (administered by DAAD) is thankfully acknowledged.

Appendix. The Mellin transform technique and Fox H-function

In many cases the transformations from the harmonic response functions $G^*(\omega)$ and $J^*(\omega)$ to the step responses $G(t)$ and $J(t)$ (cf equations (17), (18) and (20)) are not tabulated. Here the knowledge of the Mellin transform (cf equation (30)) is of much help. The Mellin transform obeys the functional relation [35]

$$\mathcal{M}\{x^\nu f(ax^p); z\} = p^{-1}a^{-(z+\nu)/p}\hat{f}\left(\frac{z+\nu}{p}\right) \tag{A1}$$

with $a, p > 0$. Equation (A1) allows one to transform certain classes of functions involving arbitrary powers of the argument and additional prefactors with power ν. Moreover, the Fourier cosine and the Mellin transform of a given function $f(x)$ are related [35]:

$$\mathcal{M}\{\mathcal{F}_C\{f(x); \omega\}; z\} = \Gamma(z)\cos\frac{\pi z}{2}\mathcal{M}\{f(x); 1-z\}. \tag{A2}$$

A similar relation holds for the Fourier sine transform [35]. Equation (A2) allows one to go from the ω domain to the Mellin domain; the inverse Mellin transformation then brings one

back to the time domain. A three-step transformation, as depicted in figure 9 is sometimes a very convenient way to perform the inverse cosine (or sine) transform $\mathcal{F}_C^{-1}$ ($\mathcal{F}_S^{-1}$).

We turn now to the evaluation of the inverse Mellin transform

$$f(x) = \mathcal{M}^{-1}\{\hat{f}(z); x\} = \frac{1}{2\pi i}\int_{c-i\infty}^{c+i\infty} dz \hat{f}(z) x^{-z}. \tag{A3}$$

The transform $\mathcal{M}^{-1}$ is intimately related to the so-called H-functions, as given by Fox in terms of a modified Mellin–Barnes integral [38]. The notation and the definition of the H-functions are

$$H_{pq}^{mn}(x) = H_{pq}^{mn}\left[x \left| \begin{matrix}(a_p, A_p)\\(b_q, B_q)\end{matrix}\right.\right] = H_{pq}^{mn}\left[x \left| \begin{matrix}(a_1, A_1), (a_2, A_2), \ldots, (a_p, A_p)\\(b_1, B_1), (b_2, B_2), \ldots, (b_q, B_q)\end{matrix}\right.\right]$$
$$= \frac{1}{2\pi i}\int_L dz \chi(z) x^z \tag{A4}$$

with the integral density

$$\chi(z) = \frac{\prod_1^m \Gamma(b_j - B_j z)\prod_1^n \Gamma(1 - a_j + A_j z)}{\prod_{m+1}^q \Gamma(1 - b_j + B_j z)\prod_{n+1}^p \Gamma(a_j - A_j z)}. \tag{A5}$$

(For constraints on the occurring parameters see e.g. [3, 38]). Note that from equation (A4) the inverse Mellin transform of a function containing products and quotients of Gamma functions is expressible in the time domain through H-functions.

We list now some very convenient properties of Fox H-functions [38].

Property 1. The H-function is symmetric with respect to the permutations of $(a_1, A_1), \ldots, (a_n, A_n)$, of $(a_{n+1}, A_{n+1}), \ldots, (a_p, A_p)$, of $(b_1, B_1), \ldots, (b_m, B_m)$ and of $(b_{m+1}, B_{m+1}), \ldots, (b_q, B_q)$.

Property 2. For $n \geqslant 1$ and $q > m$ one has

$$H_{pq}^{mn}\left[x \left| \begin{matrix}(a_1, A_1), (a_2, A_2), \ldots, (a_p, A_p)\\(b_1, B_1), (b_2, B_2), \ldots, (b_{q-1}, B_{q-1}), (a_1, A_1)\end{matrix}\right.\right]$$
$$= H_{p-1q-1}^{mn-1}\left[x \left| \begin{matrix}(a_2, A_2), \ldots, (a_p, A_p)\\(b_1, B_1), \ldots, (b_{q-1}, B_{q-1})\end{matrix}\right.\right]. \tag{A6}$$

Property 3.

$$H_{pq}^{mn}\left[x \left| \begin{matrix}(a_p, A_p)\\(b_q, B_q)\end{matrix}\right.\right] = H_{qp}^{nm}\left[\frac{1}{x} \left| \begin{matrix}(1 - b_q, B_q)\\(1 - a_p, A_p)\end{matrix}\right.\right]. \tag{A7}$$

Property 4. For $k > 0$

$$H_{pq}^{mn}\left[x \left| \begin{matrix}(a_p, A_p)\\(b_q, B_q)\end{matrix}\right.\right] = kH_{pq}^{mn}\left[x^k \left| \begin{matrix}(a_p, kA_p)\\(b_q, kB_q)\end{matrix}\right.\right]. \tag{A8}$$

Property 5.

$$x^\sigma H_{pq}^{mn}\left[x \left| \begin{matrix}(a_p, A_p)\\(b_q, B_q)\end{matrix}\right.\right] = H_{pq}^{mn}\left[x \left| \begin{matrix}(a_p + \sigma A_p, A_p)\\(b_q + \sigma B_q, B_q)\end{matrix}\right.\right]. \tag{A9}$$

An H-function may be written in terms of an alternating power series [38], a fact which is convenient for computations. As an example, for H_{12}^{11} this results in

$$H_{12}^{11}\left[x \left| \begin{matrix}(a, A)\\(a, A); (0, 1)\end{matrix}\right.\right] = A^{-1}\sum_{k=0}^{\infty} \frac{(-1)^k x^{(k+a)/A}}{\Gamma(1 + (k + a)/A)} \tag{A10}$$

from which one finds the following rule for the differentiation of H_{12}^{11}:

$$\frac{d}{dx} H_{12}^{11}\left[x \left| \begin{matrix}(a, A)\\(a, A); (0, 1)\end{matrix}\right.\right] = H_{12}^{11}\left[x \left| \begin{matrix}(a - A, A)\\(a - A, A); (0, 1)\end{matrix}\right.\right]. \tag{A11}$$

Now the series in (A10) does not converge fast for large values of x. Thus it is important to have property 3 at hand, which allows one to rewrite H_{12}^{11} as a function of $1/x$, from which a series in $1/x$ follows, by help of (A10). We have

$$H_{21}^{11}\left[\frac{1}{x}\,\middle|\,\begin{matrix}(1-a,A);(1,1)\\(1-a,A)\end{matrix}\right]=A^{-1}\sum_{k=0}^{\infty}\frac{(-1)^k(1/x)^{(k+1-a)/A}}{\Gamma(1-(k+1-a)/A)}. \tag{A12}$$

This allows the numerical evaluation of H_{12}^{11} for large x-values.

The behaviour for small and large x follows immediately from the power series (A10) and (A12):

$$AH_{12}^{11}\left[x\,\middle|\,\begin{matrix}(a,A)\\(a,A);(0,1)\end{matrix}\right]\cong\frac{1}{\Gamma(1+a/A)}x^{a/A} \tag{A13}$$

for $x \ll 1$ and

$$AH_{12}^{11}\left[x\,\middle|\,\begin{matrix}(a,A)\\(a,A);(0,1)\end{matrix}\right]\cong\frac{1}{\Gamma(1+(a-1)/A)}x^{(a-1)/A} \tag{A14}$$

for $x \gg 1$.

Throughout this paper we use the symbol $\cong$ to mean 'asymptotically equivalent'.

References

[1] Blumen A, Klafter J and Zumofen G 1986 *Optical Spectroscopy of Glasses* ed I Zschokke (Dordrecht: Reidel)
[2] Ngai K L 1987 *Non-Debye Relaxation in Condensed Matter* ed T V Ramakrishnan and L Raj Lakshmi (Singapore: World Scientific)
[3] Glöckle W G and Nonnenmacher T F 1991 *Macromolecules* **24** 6426
[4] Metzler R, Nonnenmacher T F and Kilian H-G 1995 *J. Chem. Phys.* **103** in press
[5] Friedrich C and Braun H 1992 *Rheol. Acta* **31** 309
[6] Chambon F and Winter H H 1987 *J. Rheol.* **31** 683
[7] Scanlan J C and Winter H H 1991 *Macromolecules* **24** 47
[8] Schiessel H and Blumen A 1995 *Macromolecules* **28** 4013
[9] Scher H and Montroll E W 1975 *Phys. Rev.* B **12** 2455
[10] Schnörer H, Domes H, Blumen A and Haarer D 1988 *Phil. Mag. Lett.* **58** 101
[11] Armstrong R D and Burnham R A 1976 *J. Electroanal. Chem.* **72** 257
[12] Cole K S and Cole R H 1941 *J. Chem. Phys.* **9** 341
[13] Jonscher A K 1977 *Nature* **267** 673
[14] Kjartansson E 1979 *J. Geophys. Res.* **84** 4737
[15] Doi M and Edwards S F 1986 *The Theory of Polymer Dynamics* (Oxford: Clarendon)
[16] Friedrich C 1991 *Rheol. Acta* **30** 151
[17] Nonnenmacher T F and Glöckle W G 1991 *Phil. Mag. Lett.* **64** 89
[18] Kuiken G D C 1994 *Thermodynamics of Irreversible Processes* (Chichester: Wiley)
[19] Glöckle W G and Nonnenmacher T F 1994 *Rheol. Acta* **33** 337
[20] Schiessel H and Blumen A 1993 *J. Phys. A: Math. Gen.* **26** 5057
[21] Schneider W R and Wyss W 1989 *J. Math. Phys.* **30** 134
[22] Metzler R, Glöckle W G and Nonnenmacher T F 1994 *Physica* **211A** 13
[23] Hilfer R and Anton L 1995 *Phys. Rev.* E **51** R848
[24] Hilfer R 1995 *Fractals* **3** 211
[25] Ward I M 1983 *Mechanical Properties of Solid Polymers* (Chichester: Wiley)
[26] Tschoegl N W 1989 *The Phenomenological Theory of Linear Viscoelastic Behavior* (Berlin: Springer)
[27] Oldham K B and Spanier J 1974 *The Fractional Calculus* (New York: Academic)
[28] Miller K S and Ross B 1993 *An Introduction to the Fractional Calculus and Fractional Differential Equations* (New York: Wiley)
[29] Schiessel H, Alemany P and Blumen A 1994 *Progr. Colloid Polym. Sci.* **96** 16
[30] Heymans N and Bauwens J-C 1994 *Rheol. Acta* **33** 210
[31] Blizard R B 1951 *J. Appl. Phys.* **22** 730
[32] Schiessel H, Oshanin G and Blumen A 1995 *J. Chem. Phys.* **103** (12) in press

[33] Gradshteyn I S and Ryzhik I M 1965 *Table of Integrals, Series and Products* (New York: Academic)
[34] Nonnenmacher T F 1991 *Rheological Modelling: Thermodynamical and Statistical Approaches (Lecture Notes in Physics 381)* ed J Casas-Vázquez and D Jou (Berlin: Springer)
[35] Oberhettinger F 1974 *Tables of Mellin Transforms* (Berlin: Springer)
[36] Erdélyi A (ed) 1955 *Bateman Manuscript Project, Higher Transcendental Functions* vol III (New York: McGraw-Hill)
[37] Wolf K B 1979 *Integral Transforms in Science and Engineering* (New York: Plenum)
[38] Mathai A M and Saxena R K 1978 *The H-function with Applications in Statistics and Other Disciplines* (New Delhi: Wiley Eastern)
[39] Gross B 1947 *J. Appl. Phys.* **18** 212